Journal of the Korea Concrete Institute
Vol.16 No.6, pp.867~873, December, 2004

An Experimental Study to Prevent Debonding Failure of Full-Scale RC Beam Strengthened with Multi-Layer CFS

Young-Chan You[1)*], Ki-Sun Choi[1)], and Keung-Hwan Kim[1)]

[1)] *Building Research Division, Korea Institute of Construction Technology, Korea*

(Received February 5, 2004; Accepted September 30, 2004)

Abstract

It has been known that debonding failures between CFS(Carbon Fiber Sheet) and concrete in the strengthened RC beams are initiated by the peeling of the sheets in the region of combined large moment and shear forces, being accompanied by the large shear deformation after flexural cracks. These shear deformation effects are seldom occurred in small-scale model tests, but debondings due to the large shear deformation effects are often observed in a full-scale model tests. The premature debonding failure of CFS, therefore, must be avoided to confirm the design strength of full-scale RC beam in strengthening designs.

The reinforcing details, so- called 'U-Shape fiber wrap at mid-span' which wrapped the RC flexural members around the webs and tension face at critical section with CFS additionally, were proposed in this study to prevent the debonding of CFS. Other reinforcing detail, so called 'U-Shape fiber wrap at beam end' were included in this tests and comparisons were made between them.

Keywords: CFRP(carbon fiber reinforced polymer), CFS(carbon fiber sheet), strengthening, peeling, debonding failure, U-shape wrap, full-scale RC beam

1. Introduction

Many studies on the developments of the new strengthening materials and method have been conducted both in Japan and Europe in recent decades. Also, the demand of strengthening technologies for the RC structures with CFS(Carbon Fiber Sheet) have been increased rapidly owing to its easy applications and economic point of view in domestic areas. According to these trends, the relevant experiments and studies have been conducted since middle 1990's in Korea.

Many tests have revealed the various types of failure modes of FRP-strengthened RC beams.[1-4)] The failure criteria can be grouped in six major categories; 1) rupture of FRP, 2) concrete compression failure, 3) concrete shear failure at point of FRP terminate. 4) delamination of concrete and FRP layer along the re-bar, 5) debonding between FRP and concrete, 6) peeling of FRP due to flexural shear crack. Among the failure criteria, 6th failure mode seldom occurs in small scale model tests, which leads frequent ignorance of its importance in the strengthening design of RC beams by FRP.

These failure modes can be observed in the region of combined large flexural moment and shear forces such as concentrated loading point. Peeling of FRP sheets or plates starts due to the increased and concentrated shear deformation after flexural crack occurs. In this case, general reinforcing details proposed in the previous studies,[6)] are not appropriate, which only tries to ensure bonding force by determining the length of sheets or plates considering the bonding stresses.

The purpose of this study is to investigate the peeling mechanism of CFS in the strengthened RC beams. A reinforcing detail to prevent the peeling of CFS is also suggested, which would be the basic guidelines for the strengthening design and construction of externally bonded CFS system.

* *Corresponding author*
Tel.: +82-031-910-0364 Fax.: +82-031-910-0361
E-mail address: ycyou@kict.re.kr

2. Scope

As was mentioned previously, failure mechanisms of RC beam strengthened with FRP are generally classified in six groups from many experimental results. Among the failure mechanisms, peeling of FRP due to the flexural shear cracks has been observed especially in full or large-scale model tests. Main factors influencing the peeling of CFS are existing shear reinforcement, laminate bonded length, relative stiffness of laminate to member, adherent, concrete and strengthening material.[3] Unlike the strengthening with the steel plates for flexural members, it has been recognized that peeling of CFS at mid-span initiates prior to at the beam end especially in case of the thin or long FRP.[2-5]

Mid-span peeling, however, has been seldom observed in a small-scaled model test, and the significance of the phenomenon was often ignored consequently. This is mainly because those beams were tested with 4-point loading and there was a certain limitation for the span length of laminate in a small-scale model test. The peeling mechanism of CFS at mid-span in the strengthened beam subjected to large moment and shear simultaneously is shown in Fig. 2. After flexural cracks occurred, it is extended toward the loading point due to the shear stress. As the applied load is increased, shear deformation is concentrated on the crack

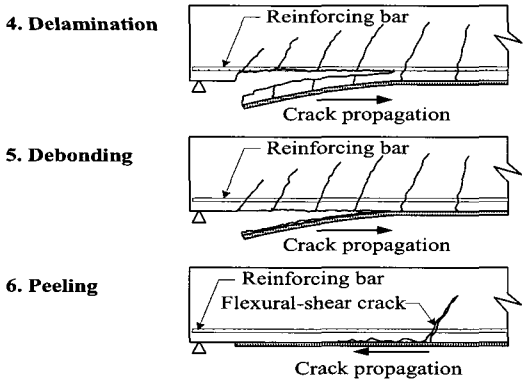

Fig. 1 Failure modes of FRP-plated RC beam [10]

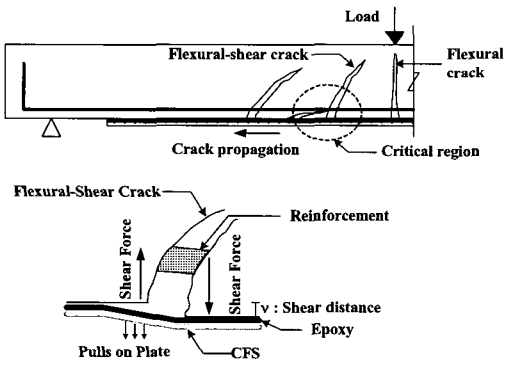

Fig. 2 Mid-span peeling mechanism due to large flexural-shear crack

point and vertical shear deflection increases which induces the peeling force to the laminates. In case that a beam is subjected to uniformly distributed loads, such mid-span peeling seldom occurs. But in a real building structure, a girder is often subjected to concentrated load at mid-span from intermediate beams. In this case, such girder should be reinforced to prevent mid-span peeling caused by the combined high moment and shear forces.

In this study, series of full-scaled RC beams strengthened with CFS by different types of reinforcing details were tested to investigate the validity and effect of each detail. Test details include 'U-shape fiber wrap' wrapping both sides of web and bottom face of beam at mid-span or beam end. RC beams without U-shaped wrap were also tested whose bonded length of CFS was designed based on the allowable bond stress $\tau_a = 0.8\ N/mm^2$, $\tau_a = 0.6\ N/mm^2$. The bond stresses were derived from the previous small-scale model tests.[6,8]

3. Experimental program

3.1 Material tests

Air-entrained concrete with specified compressive strength of 24.0MPa was supplied by a local ready-mix batch plant. Type I portland cement and 25mm nominal maximum size coarse aggregate were used. Compression cylinders measuring φ100×200mm are prepared for each specimen. The material test for high strength 200g/m^2 CFS produced by domestic manufacturer in Korea were carried out. Tensile properties as well as mechanical properties of CFS and epoxy resin were obtained according to the standard test procedure of JIS K 7073. The width and length of tensile test specimen are 12.5mm and 200mm, respectively. Also, GFRP taps with 1.5mm thickness were attached at each end of test specimen. Tables 1~4 show the test results of the each materials.

3.2 Full-scale RC beam tests

3.2.1 Test specimen

Six beam specimens were tested including standard test model. The standard test model, which simulates a typical beam in an ordinary office building was not strengthened with CFS. 5-D22 was placed for tensile reinforcement and 3-D19 for compression. D10@100 stirrups were employed to prevent shear failure prior to flexural yielding. Two layers of 200g/m^2 CFS were attached to the strengthened test models. General configurations of test specimens are shown in Fig. 3 and detailed characteristics of reinforcing bars and strengthening materials are summarized in Table 5.

Table 1 Material properties of concrete

Curing age	Tensile strength (MPa)	Compressive strength (MPa)	Young's modulus (GPa)
32 days	2.34	32.7	27.1

Table 2 Material properties of reinforcing bar

Bar size	Yield strength (MPa)	Young's modulus (GPa)	Tensile strength (MPa)	Elongation (%)
D10	366.1	176.0	562.0	28
D19	386.0	146.0	627.0	14
D22	375.4	159.0	576.0	19

Table 3 Material properties of CFS (t_{cf}=0.111mm)

Classification	Tensile strength (MPa)	Young's modulus (GPa)	Failure strain
Nominal	3,550.0	235.0	0.0151
Test	4,513.4	259.0	0.0170

Table 4 Material properties of epoxy resin unit : MPa

Classification	Compressive strength	Tensile strength	Flexible strength	Shear strength
Nominal	70.0	30.0	40.0	10.0
Test	64.7	32.0	49.0	11.0

Table 5 Details of reinforcing bar and strengthening CFS

Specimen	Reinforcement	Layer (ply)	Bond Length (mm)	Remark
RS		-	-	Control
RF2-B3		2	2,000	Soffit
RF2-UCB3	A'_s= 861 mm^2	2	2,000	Soffit + Center U-wrap
RF2-B2	A_s=1,935 mm^2	2	2,700	Soffit
RF2-UCB2	ρ/ρ_b=0.3	2	2,700	Soffit + Center U-wrap
RF2-UEB2		2	2,700	Soffit + End U-wrap

A'_s : area of top bar
A_s : area of bottom bar
ρ : reinforcement ratio
ρ_b : reinforcement ratio at balanced failure

The bonding length of CFS for the specimens RF2-B3 and RF2-UCB3 were calculated based on Formula (1). The bond stress between concrete and CFS was chosen as $\tau_a = 0.8\ \mathrm{N/mm^2}$, which was proved safe enough from the previous small-scaled model tests. On the other hands, that of the specimen RF2-B2, RF2-UCB2 and RF2-UEB2 is based on the bond stress of $\tau_a = 0.6\ \mathrm{N/mm^2}$. All of the specimens were tested with 3-point loading. Both of RF2-UCB2 and RF2-UCB3 specimens were additionally

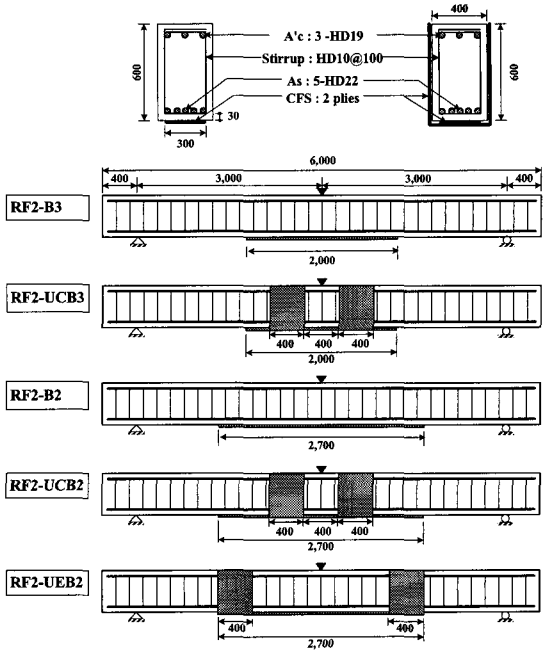

Fig. 3 Details and dimensions of test specimens

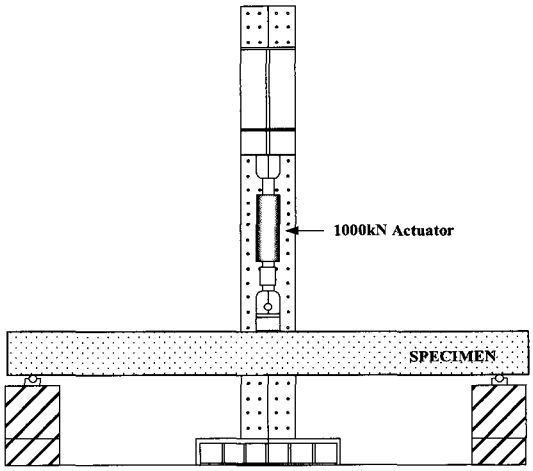

Fig. 4 Specimen test set-up

strengthened with U-shaped CFS wrap at near the mid-span loading point, while RF2-UEB2 at each end of CFS.

$$l = \frac{f_{cf} \cdot n \cdot t_{cf}}{\tau_a} \tag{1}$$

τ_a : design bond stress of CFS to concrete
f_{cf} : design tensile strength of CFS
n : layer of CFS, t_{cf} : nominal thickness of CFS

3.2.2 Test set-up

3-point load is applied at the center of beam specimen using the hydraulic actuator whose permissible capacity is 1000 kN which was set-up at the loading frame as shown in Fig. 4.

As the measuring devices, two units of 200mm LVDT were settled for the measurement of deflection at mid-span. Ten units of strain gage type transducer (PI Displacement Transducer) were settled at 60mm intervals vertically at central region of the beam to obtain the sectional strain gradient. Two units of WSG(wire strain gage) were attached on CFS at mid-span. For the specimen with U-type strengthening details, the WSGs were attached in fiber direction to measure the CFS strain. Fig. 5 shows the location of each measuring apparatus.

4. Test results

4.1 Failure mode

Fig. 6 represents the load-deflection relationship of specimens whose failure was governed by debonding of CFS. Comparison of experimental results and theoretically computed values are listed in Table 6. Load-deflection behavior of specimen RS which is not strengthened with CFS shows the typical flexural failure modes of RC beam. On the other hands, peeling of CFS initiated at mid-span was observed in both RF2-B3 and RF2-B2 specimens. The failure strains of CFS and maximum loads were different with each other. RF2-B3 and RF2-B2 specimens were strengthened with CFS at the soffit of the beam with the bonded length of 2,000mm and 2,700 mm respectively.

In the case of specimen RF2-B3, peeling was initiated at the point of 200mm from mid-span due to the flexural shear crack and propagates to both ends rapidly, which finally leads to debonding failure of CFS. Final strain of CFS at mid-span of beam was $6{,}129\times 10^{-6}$ which is 40% of the manufacturer's specified failure strain. Maximum load was 348.9kN which is 132% of the nominal strength of the unstrengthened specimen.

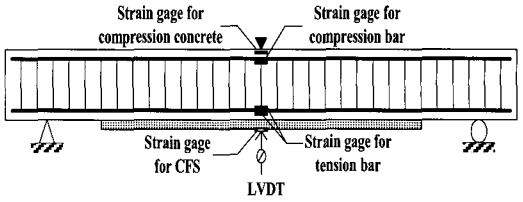

Fig. 5 Location of measurement apparatus

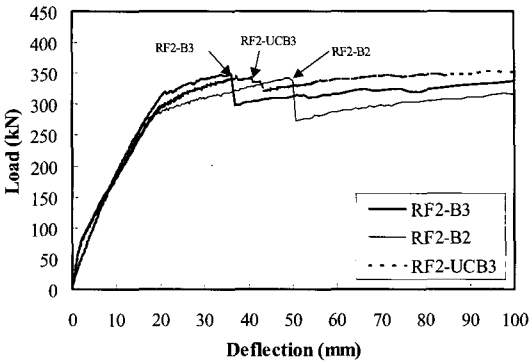

Fig. 6 Load-deflection curve of the specimens with debonding failure of CFS

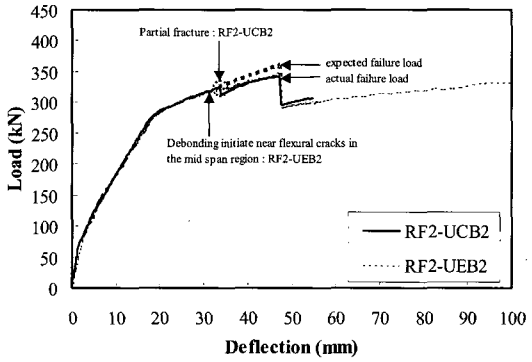

Fig. 7 Load-deflection curve of the specimens with U-shape fiber wrap at mid-span

Table 6 Comparison of calculated and experimental results

Specimen	Yield load(kN)		Max. load(kN)		δ_f (mm)	ε_c ($\times 10^{-6}$)	ε_{cf} ($\times 10^{-6}$)	Failure mode
	Cal_n	Exp	Cal_n	Exp				
RS	252.6	284.5	264.7	312.7	76.90	3,000	-	Concrete crushing after tensile bar yielding
RF2-B3	264.4	308.9	346.8	348.9	36.06	2,070	6,129	Debonding caused by peeling started at mid- span
RF2-UCB3	264.4	277.2	346.8	342.2	40.58	1,898*	6,643	Debonding started from outside U-wrap
RF2-B2	264.4	285.1	346.8	344.0	48.88	1,904*	9,967	Debonding started at mid span
RF2-UCB2	264.4	270.6	346.8	342.4	48.84	3,568	10,564	CFS rupture at mid span
RF2-UEB2	264.4	278.1	346.8	347.9	47.00	3,476	9,010	CFS rupture within end U-wrap after debonding started at mid span

* : Maximum strain which is experimentally measured

ε_c : Concrete strain at CF sheets rupture (ultimate state)

ε_{cf}: CF sheet strain at CF sheet rupture (ultimate state)

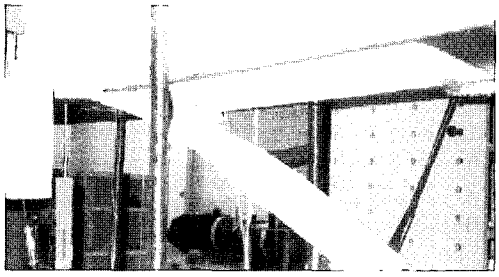

Fig. 8 Specimen RF2-B3 at failure (debonding)

Fig. 9 Specimen RF2-UCB3 at failure (debonding)

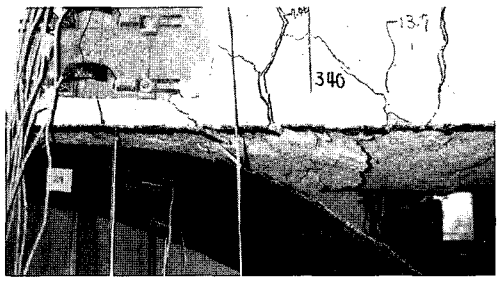

Fig. 10 Specimen RF2-B2 at failure (debonding)

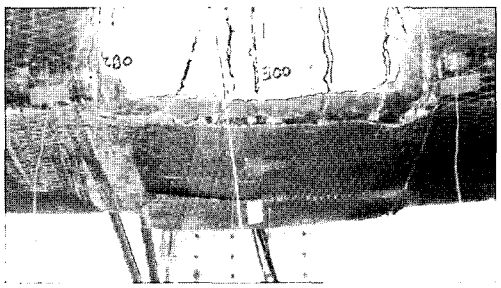

Fig. 11 Specimen RF2-UCB2 at failure (rupture)

Fig. 12 Specimen RF2-UEB2 at failure (rupture after debonding started at mid-span)

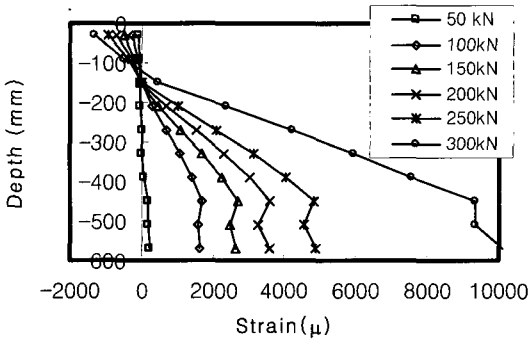

Fig. 13 Sectional strain gradient of typical specimen

In the case of RF2-UCB2 specimen, which was additionally strengthened with U-shape CFS at the critical section near mid-span of beam, slight debonding between CFS and concrete at the soffit of the beam was observed at the load level of 289 kN which seems to be initiated due to the surface roughness taken place during manufacturing. But no further apparent peeling did not occur because of the confining effects of the U-shape fiber wrap. At that time, some part of longitudinal CFS was ruptured, but the loss of load bearing capacity was not critical. Finally, remaining parts of CFS were ruptured at the load level of 342.4kN. Strain of CFS at mid-span was $10{,}564\times 10^{-6}$ or 70% of the specified failure strain and maximum load was 129% of the unstrengthened beam. In RF2-UEB2 specimen with U-shape wrap at both beam ends, peeling was started at near mid-span and propagates to ends. CFS ruptured at the point of U-shape wrap and the failure load was 347kN. Failure strain of CFS at actual failure was $9{,}010\times 10^{-6}$ which is 60% of the manufacturer specified failure strain. Maximum load was 131% that of the unstrengthened beam. In RF2-UCB3 specimen, debonding starts from outside of U-wrap, which leads debonding of CFS finally.

4.2 Sectional strain gradient

Fig. 13 shows the sectional strain gradient obtained from ten units of PI displacement transducers which were settled at 60mm intervals on the beam web as shown in Fig. 5.

The sectional strain distribution appears to be a linear before yielding of reinforcing bar, but strain of reinforcing bar tends to be greater than that of CFS after yielding. It means that some slips are expected to be happened between concrete tensile fiber and CFS. From that point of view, an actual distance from extreme compression fiber to neutral axis is always smaller then that theoretically computed by linear strain distribution, which results in conservative estimations.

4.3 Shear deformation

U-shaped fiber wrap details were proved to be effective in increasing the shear strength of RC beam in the previous studies. However, peeling of CFS can be taken place at point of combined high moment and shear forces even though the beam has enough shear strength. This implies that bond failure can be occurred in a beam strengthened by CFS with sufficient bonded lengths. Fig. 14 shows the typical crack pattern at failure in this test. There are apparent flexural-shear cracks from near loading point, which failed by peeling of CFS. Even though RF2-UEB2 beam which is U-wrapped at ends of laminate failed by rupture of CFS, peeling was initiated near at loading point due to flexural-shear crack development. RF2-UCB2 with U-wrap at loading point, which failed by rupture of CFS without any peeling, shows the best behavior and the strengthening details are considered effective to prevent premature debonding.

4.4 Examination of strengthening effects by CFS

Previous studies estimated the strengthening effects of FRP on the basis of the strength difference between the maximum flexural capacity of strengthened members and the nominal flexural capacity of non-strengthened members by theoretical analysis(see Fig.15①). But this method has the possibilities to overestimate the strengthening effects by FRP because probable flexural moment of RC members was comprised in the maximum flexural capacity of the strengthened beams (see Fig.15②). For this reason, we apply the processes as shown in (a)~(d) to obtain the real load increments by CFS strengthening. The process of calculation is as follows.

$$\Delta P_{cf} = P_u - P_s \quad (2), \qquad \Delta M_{cf} = \Delta P_{cf} \times \frac{L}{4} \quad (3)$$

$$f_{cf} = \frac{\Delta M_{cf}}{Z} \quad (4), \qquad \varepsilon_{cf\text{-}cal} = \frac{f_{cf}}{E_{cf}} \quad (5)$$

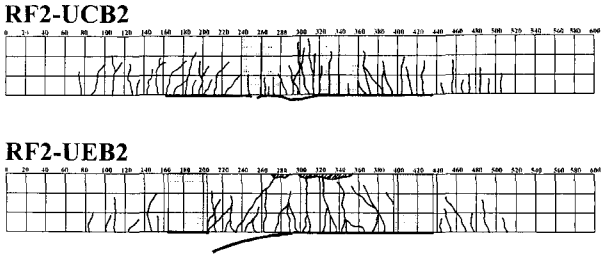

Fig. 14 Typical crack pattern at failure

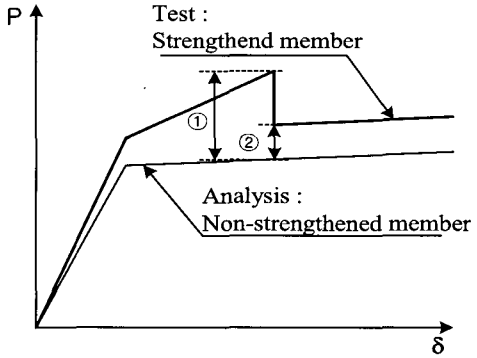

Fig. 15 Probable strength calculation of RC beams

(a) Calculate the strength increment (ΔP_{cf}) from the difference between the maximum load by strengthening (P_u) and the decreased load (P_s) at CFS rupture.
(b) Calculate the moment increment (ΔM_{cf}) from (a).
(c) Calculate the tensile stress (f_{cf}) at CFS rupture by sectional analysis.
(d) Calculate the strain ($\varepsilon_{cf\text{-}cal}$) by dividing the tensile stress of (c) by the elasticity modulus of CFS.

The specific values computed by the procedures of (a)~(d) explained above are shown in Table 7. As shown in Table 7, the ultimate strains calculated by these procedures are almost similar to those measured at each specimen. Thus, all the measured data and the evaluation for strengthening effects by CFS are considered very reliable.

Table 7 Tensile stress and measured strain of CFS

Specimen	Layer (ply)	P_u (kN)	P_s (kN)	ΔP_{cf} (kN)	ΔM_{cf} (kN·m)	T_{cf} (kN)	f_{cf} (N/mm^2)	$\varepsilon_{cf\text{-}cal}$ (μ)	$\varepsilon_{cf\text{-}sg}$ (μ)	f_{cf}/f_{cfn}
RF2-B3	2	348.9	302.3	46.6	69.9	125.50	1884.3	8,018	6,129	0.53
RF2-UCB3	2	342.2	320.7	21.5	32.3	58.35	876.1	3,728	6,643	0.25
RF2-B2	2	344.0	287.3	56.7	85.1	155.06	2328.3	9,907	9,967	0.66
RF2-UCB2	2	342.4	295.3	47.1	70.7	129.81	1949.2	8,294	10,564	0.55
RF2-UEB2	2	347.9	293.4	54.5	81.8	151.39	2273.2	9,673	9,010	0.64

P_u : maximum load before CFS rupture
P_s : decreased load after CFS rupture
ΔP_{cf} : load difference before and after CFS rupture
ΔM_{cf} : moment difference before and after CFS rupture
T_{cf} : tensile force of CFS calculated as $\Delta M_{cf}/Z$
f_{cf} : tensile stress of CFS calculated as T_{cf}/A_f

4.5 Bond stress

The final failure of the specimen RF2-UCB3 designed based on the bond strength of $\tau_a = 0.8\ N/mm^2$ was governed by peeling CFS, even though it was reinforced additionally by U-wrap at critical region. However, the CFS rupture was observed in the specimen of RF2-UCB2 whose design bond stress was $\tau_a = 0.6\ N/mm^2$ without any slight peeling of CFS up to failure. Also, this experimental study shows that there is an apparent peeling phenomenon in the region of combined large flexural moment and shear forces in the case of the specimen RF2-UEB2 even though it is finally failed by rupture of CFS.

Therefore, the bond stress of $\tau_a = 0.8\ N/mm^2$ are not enough to insure the FRP rupture failure even though U-shape wrapping at critical region was adopted. Design bond stress of $\tau_a = 0.6\ N/mm^2$ was recommended to confirm the CFS rupture failure. Also, the RC beams strengthened by CFS must be reinforced by U-shape wrapping at critical sections to prevent the reduction of flexural capacity due to premature peeling of CFS.

5. Conclusions

Full-scale model tests were conducted to investigate the validity of suggested FRP reinforcing details by U-shape fiber wrapping additionally at mid-span to prevent debonding failure of RC beams strengthened by multi-layer CFS. Also, the design bond stresses between CFS and concrete were examined. From this study, following conclusions are obtained.

1) Unlike the small-scaled model, peeling of CFS starting at flexural shear crack occurs in full-scale beam strengthened by CFS. U-shaped fiber wrapping at critical region is effective in controlling flexural shear crack and preventing debonding failures.
2) Full scaled specimen designed based on bond stress of $\tau_a = 0.6\ N/mm^2$ is failed by rupture of CFS, while specimen of $\tau_a = 0.8\ N/mm^2$ by debonding failure, even though it was reinforced by U-wrap additionally. So, minimum bond strength of CFS to concrete should not be greater than $\tau_a = 0.6\ N/mm^2$.
3) 'U-shape fiber wrap' is more effective when it is employed at near loading point rather than at beam ends of CFS.

Acknowledgement

This paper is a part of the research project named "Performance Evaluation of Repairing and Strengthening for RC Building Structure." Support for this research by '99 National R&D Program for Construction and Transportation Technology under Grant No. R&D/99-building07 is greatly acknowledged.

References

1. Choi, K. D., et al, "Bond between CFS and Concrete," *Fall Conference, KCI*, Vol.12, No.2, 2000, pp.1019~1024.
2. Arduini, M. and Nanni, A., "Behavior of Pre-cracked RC Beams Strengthened with Carbon Fiber Sheets," *Journal of Composite for Construction, ASCE*, Vol.1, No.2, 1997, pp.63~70.
3. Buykozturk, O. and Hearing B., "Failure Behavior of Precracked Concrete Beams Retrofitted with FRP," *Journal of Composite for Construction*, ASCE, Vol.2, No.3, 1998, pp.138~144.
4. Rahimi, H. and Hutchinson, A., "Concrete Beams Strengthened with Externally Bonded FRP Plates," *Journal of Composite for Construction, ASCE*, Vol.5, No.1, 2001, pp.44~56.
5. Sebastian, W. M., "Significance of Midspan Debonding Failure in FRP-Plated Concrete Beams," *Journal of Structural Engineering, ASCE*, Vol.127, No.7, 2001, pp.792~798.
6. Hankook Fiber/Carbon Co., "Technical Data for CF sheet Method(II)," Hankook Fiber/Carbon Co., HaeLim, 1998, pp.52~53.
7. Concrete Committee, JSCE, "*Guideline of Retrofitting of Concrete Structures (Preliminary Reports)*," JSCE, 1999, pp.88~97.
8. MOCT, KICT, "*Study for Evaluation of Repair and Retrofit Method for Reinforced Concrete Structures*," MOCT, KICT , 2000, pp.220~241.
9. ACI COMMITTEE 440, "*Guide for the Design and Construction of Externally Bonded FRP System for Strengthening Concrete Structure*," 2002, pp.21~25.
10. Teng, J.G., Chen, J.F., Smith, S.T., and Lam, L., "FRP Strengthened RC Structures," Wiley, 2002, pp.31~46.